Cellular Signalling 53 (2019) 162–169

Contents lists available at ScienceDirect

Cellular Signalling

journal homepage: www.elsevier.com/locate/cellsig

Loss of hypermethylated in cancer 1 (HIC1) promotes lung cancer progression

Yue Li[a,1], Mengfei Yao[b,1], Tianqi Wu[b], Liyan Zhang[c], Yingying Wang[d], Liang Chen[e], Guohui Fu[a], Xiaoling Weng[b,*], Jianhua Wang[b,f,*]

[a] Department of Pathology Center, Shanghai General Hospital/Faculty of Basic Medicine, Shanghai Jiao Tong University School of Medicine, Shanghai, China
[b] Cancer institute, Fudan University, Shanghai Cancer Center, Shanghai, China
[c] Department of Neurology, Beijing Friendship Hospital, Capital University of Medical Sciences, China
[d] Department of Biochemistry and Molecular and Cell Biology, Shanghai Jiao Tong University School of Medicine, Shanghai, China
[e] National Institute of Biological Sciences (NIBS), Beijing, China
[f] School of Medicine, Anhui University of Science & Technology, Huainan, Anhui, China.

ARTICLE INFO

Keywords:
HIC1
Lung cancer
DNA repair pathway
Tumorigenesis

ABSTRACT

Lung cancer is a leading cause of cancer mortality worldwide with dramatically increasing incidence in recent years. However, the mechanism underlying its progression remains unclear. The aim of this study was to identify the role of hypermethylated in cancer 1 (HIC1) in lung cancer development. Here we found that HIC1 expression was markedly decreased in lung cancer compared with the corresponding adjacent non-cancerous tissues. Meanwhile, overall survival (OS) of lung cancer patients was negatively related with HIC1 expression using TCGA and GEO datasets. Loss of HIC1 expression promoted cell proliferation and migration *in vitro*. Notable, HIC1 knock-out in $Kras^{G12D/+(Lox\text{-}Stop\text{-}Lox)}$/sgHIC1 mice had remarkable effect on tumorigenesis compared with $Kras^{G12D/+(Lox\text{-}Stop\text{-}Lox)}$/sgTd control mice. Mechanistic analyses showed that ADAMTS9, DCDC2, FAM46C, ZNF883, F2R, MSH6 and PAX2 genes may be potential downstream targets; DNA repair pathway and transcriptional regulation by TP53 pathway were involved. Finally, this study reveals that HIC1 is associated with lung cancer progression and may provide an effective strategy for its treatment.

1. Introduction

Lung cancer is one of the most common malignant tumors and is the leading cause of cancer mortality worldwide [1,2]. Lung tumors are divided into two histological types: 85% of lung cancer cases are classified as non-small cell lung cancer (NSCLC),the most common and aggressive type, the rest (15%) are classified as small cell lung cancer (SCLC) [3]. Despite advances in radio- and chemotherapy and development of new molecular-targeted drugs, the overall 5-year survival of lung cancer remains poor [4]. Therefore, identifying the mechanism underlying the progression of lung cancer may be beneficial for its prognosis and treatment.

Hypermethylated in cancer 1 (HIC1) is identified as a tumor suppressor gene located at chromosome 17p13.3 close to telomeric TP53 [5]. HIC1 is a sequence-specific zinc finger repressor and has three known functional regions, the N-terminal BTB/POZ domain, the central region and the C-terminal DNA binding domain [6]. The BTB/POZ domain is responsible for protein–protein interaction which is crucial for its biological function, while the C-terminal Zinc Fingers domains are involved in sequence-specific binding to a HIC1-responsive element (HiRE) with a TGCC(A/C) core motif [7]. It has been reported that epigenetic gene silencing of *Hic1* is one of the most common events in human cancer [8–10]. Consistently, conventional knockout mice with homozygous deletion of HIC1 was died, followed by mid-gestation embryonic lethality [11], whereas heterozygous mutants develop a range of spontaneous tumors in an age-dependent manner [12]. HIC1 is frequently inactivated by DNA hypermethylation and loss of heterozygosity in various types of human tumors, including prostate, breast, lung, liver, colorectal and gastric cancer [8–10,13,14]. Despite epigenetic silence of HIC1, several post translational regulatory mechanisms such as glycosylation, acetylation and SUMOylation [15], have been reported in several studies.

Our previous reports have indicated that loss of HIC1 in triple-negative breast cancer (TNBC) and prostate cancer may play a significant

* Corresponding authors at: Cancer institute, Fudan University Shanghai Cancer Center, 200032, China.
E-mail addresses: 3070701040@163.com (X. Weng), jianhuaw2007@qq.com (J. Wang).
[1] These authors contributed equally to this work.

https://doi.org/10.1016/j.cellsig.2018.10.006
Received 12 July 2018; Received in revised form 3 October 2018; Accepted 8 October 2018
Available online 10 October 2018
0898-6568/

role in cancer progression [10,13,14,16]. We found that HIC1 promoter was heavily methylated in NSCLC cell lines and tissues contributing to its low expression compared to normal controls. Mechanistic analyses show that autocrine secretion of IL-6 induced by loss of HIC1 activated STAT3 through IL-6/JAK pathway and was associated with NSCLC progression [8]. Here using the HIC1 knock-out in $Kras^{G12D/+(Lox\text{-}Stop\text{-}Lox)}$/sgHIC1 mice model, we further disclose the function of HIC1 in occurrence of lung cancer.

2. Materials and methods

2.1. Data mining

The profiling including HIC1 mRNA expression of lung cancers was obtained from a TCGA dataset (TCGA_LUAD_exp_HiSeqV2–2015-02-24). The HIC1 promoter methylation data was obtained from TCGA_LUAD_hMethyl450–2015-02-24. Gene Expression Omnibus (GEO) datasets GSE4573, was used to obtain the Kaplan–Meier plots with the relationship between HIC1 mRNA expression and the overall survival of lung patients.

2.2. Cell culture

Two human lung cancer cell lines (H292 and A549) and 293T embryonic kidney cells were obtained from American Type Culture Collection (ATCC). A549 and H292 were cultured in RPMI-1640 (Hyclone) supplemented with 10% fetal bovine serum and 1% PenStrep. 293 T were cultured in DMEM supplemented with 10% fetal bovine serum and 1% PenStrep. The cell lines were tested and authenticated by DNA typing in Shanghai Jiao Tong University Analysis Core and were maintained at 37 °C in a 5% CO2 atmosphere.

2.3. Construction of lentiviral vectors

The Cas9 expression constructs Lenticas9-blast and the sgRNA expression plasmid Lentiguid-puro was used to generate stable HIC1 knockout H292/A549 cell lines. Lentiviruses were produced in 293 T cells and the supernatant was collected 48 h after transfection, filtered through a 0.45-um filter, and used directly to infect tumor cells. The insert sgRNA sequences to silence HIC1 were as following: SgHIC1-1: CGCACGGAATGCACACGTACAGG, SgHIC1-2: TCTTGTCGCACGACGC GCAGCGG, SgHIC1-3: TGCGCCGAGCTGTACGCGTCGGG, SgHIC1-4: CCGCCGCGAAATGGGTCGGAAGG.

2.4. Cell colony assay

Cell colony assay was conducted by plating 500, 1000, 1500 cells per well in a TC-treated 6-well black-sided, clear bottom plate. Cells were plated as above and allowed to adhere for 2 weeks then treated with 4% formaldehyde for 30 min at room temperature, stained using coomassie brilliant blue for 30 min. Experiments were repeated at least three times.

2.5. Cell migration assay

BD Falcon cell culture inserts (8 μm) were used for cell migration assay (Cat. no.353097, BD). 5×10^4 cells suspended in 0.1 ml RPMI-1640 serum-free medium was added into the top chamber. 0.5 ml RPMI-1640 medium supplemented with 10% FBS was added to the lower chamber as a chemoattractant. After incubation for 48 h, Cells at lower surface of the inserts were fixed in 4% formaldehyde for 30 min at room temperature, stained using coomassie brilliant blue for 30 min. The migrating cells were imaged using a digital microscopy. Experiments were repeated at least three times.

2.6. Western blots analysis

Cells were washed 3 times by PBS and lysed for 30 min in radioimmunoprecipitation assay (RIPA) buffer (Cat#: 89900, Thermo Scientific, Waltham, MA) containing an anti-protease mixture (KangChen Bio-tech, shanghai, China). 20 μg of total protein was separated on a 10% SDS-PAGE, transferred to a polyvinylidene fluoride (PVDF) membrane, and probed with primary antibodies. Secondary antibodies included horseradish peroxidase (HRP) –conjugated goat-anti-mouse IgG and goat-anti-rabbit IgG secondary antibodies. The antigen-antibody reaction was visualized by enhanced chemiluminescence assay. Experiments were repeated at least three times. Primary antibody rabbit anti-HIC1 was purchased from Sigma, mouse anti-PAX2 was purchased from ABclonal. Mouse anti-GAPDH was purchased from ProteinTech.

2.7. RNA Collection and RT-qPCR

Total RNA was extracted from cells using TRIzol (Invitrogen Corp) and was reversely transcribed using the Reverse Transcriptase cDNA Synthesis Kit (Cat. no. RR037A; Taraka). Diluted cDNA was then used as templates in quantitative real-time PCR (RT-qPCR) on an Applied Biosystems 7500 Fast Real-Time PCR System (ABI, Foster, USA), using the Hidff qPCR SYBR Green Master Mix (Cat. no. 11202ES08; YEASEN) according to the manufacturer's protocol. All reactions were done in 20ul reaction volume in triplicate and the cycling conditions were 30s for 95 °C, followed by 40 cycles of 95 °C for 5 s and 60 °C for 1 min. The relative amount of mRNA was normalized to GAPDH and expressed as $2^{-\triangle\triangle Ct}$. Primers were obtained from GENEWIZ and the primer sequences were shown in Supplementary Table 1.

2.8. cDNA microarray analysis

The Agilent Human Gene Expression (8x60K, Design ID: 039494, Agilent Technologies) was used in this experiment. H292 and H292sg4, A549 and A549sg4 RNA integrity was assessed using Agilent Bioanalyzer 2100 (Agilent Technologies) and the sample labeling, microarray hybridization and raw data extration were performed according to the manufacturer's standard protocols. The threshold set for up- and down-regulated genes was a fold change ≥ 1.0.

2.9. Mice

Eight 8-10wks $Kras^{G12D/+(Lox\text{-}Stop\text{-}Lox)}$ mice with a C57BL/6 background were kindly provided by Dr. Liang Chen (National Institute of Biological Sciences (NIBS), Beijing, China). Mice were treated *via* nasal inhalation of U6-sgRNA-EFS-Cas9-2A-Cre (pSECC) lentivirus (2×10^6 p.f.u. lenti-Cre, 4 mice for sgTd and 4 mice for sgHIC1) for 10 wks. Mice were then euthanized and the entire lung were dissected out.

Three Hic1 sgRNAs were designed using CRISPRDesign to silence HIC1 as following: Hic1-gRNA1: CGTTCTTGTGCGCGCGGAAGAGG, Hic1-gRNA2: CCGCGCGCACAAGAACGTGCTGG, Hic1-gRNA3: GTTCT TGTGCGCGCGGAAGAGGG. All mice were kept under specific pathogen-free (SPF) condition and mouse care and treatment was approved by the Animal Care and Use Committee at the Shanghai Jiao Tong University. To ameliorate any suffering of mice observed throughout these experimental studies, mice were euthanized by CO2 inhalation.

2.10. Immunohistochemistry (IHC)

Mouse lungs were fixed in 4% formaldehyde overnight at room temperature and embedded in paraffin. Sections of 4 μm in thickness were used for hematoxylin–eosin (H&E) staining and immunohistochemistry. Samples were baked at 65 °C for 12 h, then deparaffinized by three 10-min extractions in 100% xylene, followed by 5-

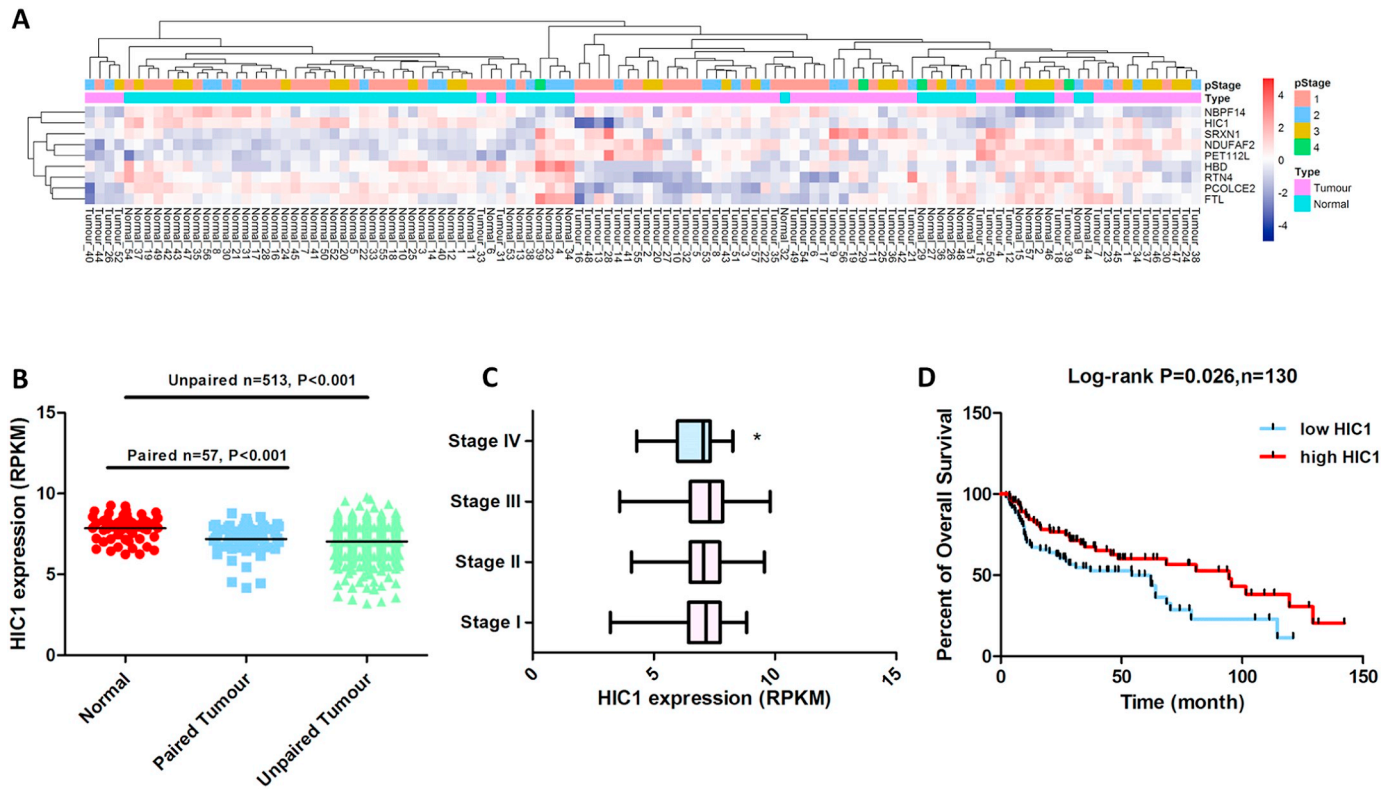

Fig. 1. Molecular features of HIC1 in lung cancer. A. The expression profiling of 9 significant genes in 57 paired normal-tumor lung cancer patients. B. HIC1 expression level in normal and tumor lung cancer patients. C. HIC1 expression level in different stages of lung cancer patients. D. Kaplan-Meier plots of the overall survival (OS) of patients stratified by HIC1 expression. *$P < .05$.

min each of descending grade of alcohol (100%, 95%, 80% and 70%). Samples were then washed briefly with phosphate-buffered saline (PBS) before transferring to boiling 10 mM sodium citrate buffer (pH 6.0) for 30 min. For immunohistochemistry, sections were pre-treated with 3% hydrogen peroxide for 10 min before blocking. Blocking was performed with 5% normal goat serum in PBS for 30 min at room temperature followed by anti-mouse HIC1 (Cat. no. bs-15485R; Bioss) incubation overnight at 4 °C. For detection with primary antibody using the immune enzymatic method, the ABC peroxidase detection system (Cat. no. PK-6105; Vector Labs) was used with 3, 3′-diaminobenzidine (DAB) as substrate (Cat. no. SK-4105; Vector Labs) according to manufacturer's instruction.

2.11. Pathway classification and enrichment analysis

The Database for Annotation, Visualization and Integrated Discovery (DAVID, http://david.abcc.ncifcrf.gov/) and Metascape (A Gene Annotation & Analysis Resource, http://metascape.org/) were used for GO and KEGG pathway analyses. GO enrichment analysis were used the Gene Ontology category (http://geneontology.org). Pathway classification within DAVID used the Kyoto Encyclopedia of Genes and Genomes database (KEGG, http://www.genome.jp/kegg/pathway.html).

2.12. Statistical analysis

The R program (http://www.r-project.org/, version 3.2.1) and GraphPad Prism 5.0 software were used for the statistical analysis. Heatmap package in R was used for the cluster of TCGA mRNA expression. The significance of the differences between the control groups and the experimental groups was evaluated using two-tailed Student's *t*-tests. The Kaplan-Meier curves for survival analyses were determined using the log-rank test. All data above represent the results obtained from triplicated independent experiments with standard errors of the mean (mean ± standard deviation (SD)). *P* value < .05 was considered significant.

3. Results

3.1. Molecular features of HIC1 in lung cancer

To evaluate the molecular landscape of HIC1 mRNA expression in lung cancer, we characterized the RNA-seq data acquired from a TCGA dataset (TCGA_LUAD_exp_HiSeqV2-2015-02-24) within 513 lung cancer patients. First, we analyzed the relationship between the mRNA expression of the 20,530 genes and the overall survival of the lung cancer patients. Then we identified 66 genes with log-rank $P < .002$ (Supplementary Table 2). The expression profiling of HIC1 and eight genes among the 66 genes was shown in 57 paired normal-tumor lung cancer patients (Fig. 1A). HIC1 promoter methylation data of 60 cpg sites was extracted from TCGA_LUAD_hMethyl450-2015-02-24 within 458 lung cancer patients. 78.3% (47/60) cpg sites were negatively correlated with HIC1 mRNA level. cg20664636 ($r = -0.1821$), cg01160692 ($r = -0.1506$) and cg25520679 ($r = -0.1310$) were the most differentially methylated sites (DMSs) (Table 1). In comparison with normal tissues, HIC1 expression level was significantly decreased in paired and unpaired tumor tissues (Fig. 1B). Meanwhile, we observed that HIC1 expression level was lower in stage IV than in stage I-III ($P < .05$ between stage IV and stage III, Fig. 1C). Furthermore, Kaplan–Meier plots obtained from the GEO datasets GSE4573 indicated that lower HIC1 expression was associated with shorter overall survival among lung patients ($P < .05$, Fig. 1D).

Table 1
Pearson's correlation coefficients of HIC1 cpg sites methylation level and HIC1 expression.

TargetID	Methylation level	r	t	P value	CHROMOSOME_36	COORDINATE_36	UCSC_REFGENE_NAME	UCSC_REFGENE_ACCESSION	UCSC_REFGENE_GROUP	UCSC_CPG_ISLANDS_NAME	RELATION_TO_UCSC_CPG_ISLAND
cg00138101	−0.082 ± 0.0742	−0.0780	−1.6565	0.09833	17	1907859	HIC1;HIC1	NM_001098202;NM_006497	Body;Body	chr17:1952919-1962328	Island
cg00592510	−0.334 ± 0.090	**−0.1181**	**−2.5175**	**0.01217**	17	1904375	HIC1	NM_006497	TSS1500	chr17:1952919-1962328	Island
cg00815093	−0.434 ± 0.079	−0.0271	−0.5740	0.5662	17	1904140	HIC1	NM_006497	TSS1500	chr17:1952919-1962328	Island
cg00911794	−0.111 ± 0.0926	0.2836	6.2592	9.066E-10	17	1908882	HIC1;HIC1	NM_001098202;NM_006497	3'UTR;3'UTR	chr17:1952919-1962328	Island
cg00927777	−0.163 ± 0.121	0.0236	0.5001	0.6172	17	1906949	HIC1;HIC1	NM_001098202;NM_006497	Body;Body	chr17:1952919-1962328	Island
cg01070078	−0.443 ± 0.102	−0.0971	−2.0641	0.03959	17	1905633	HIC1;HIC1	NM_001098202;NM_006497	TSS1500;5'UTR	chr17:1952919-1962328	Island
cg01070985	−0.456 ± 0.034	0.0175	0.3711	0.7107	17	1904718	HIC1	NM_006497	TSS1500	chr17:1952919-1962328	Island
cg01143579	−0.367 ± 0.089	−0.0210	−0.4449	0.6566	17	1903708	HIC1	NM_006497	TSS1500	chr17:1952919-1962328	Island
cg01160692*	0.019 ± 0.168	**−0.1506**	**−3.2250**	**0.001352**	17	1906370	HIC1;HIC1	NM_001098202;NM_006497	1stExon;5'UTR	chr17:1952919-1962328	Island
cg01168201	−0.474 ± 0.021	−0.0203	−0.4297	0.6677	17	1905162	HIC1;HIC1;HIC1	NM_001098202;NM_006497;NM_006497	TSS1500;1stExon;5'UTR	chr17:1952919-1962328	Island
cg02151609	−0.398 ± 0.113	−0.0234	−0.4948	0.621	17	1904279	HIC1	NM_006497	TSS1500	chr17:1952919-1962328	Island
cg02376827	0.026 ± 0.116	0.0604	1.2803	0.2011	17	1908260	HIC1;HIC1	NM_001098202;NM_006497	Body;Body	chr17:1952919-1962328	Island
cg02756676	−0.440 ± 0.025	−0.0640	−1.3565	0.1756	17	1904956	HIC1;HIC1	NM_001098202;NM_006497	TSS1500;TSS200	chr17:1952919-1962328	Island
cg02964474	−0.414 ± 0.021	−0.0036	−0.0755	0.9399	17	1904752	HIC1	NM_006497	TSS1500	chr17:1952919-1962328	Island
cg03244036	−0.393 ± 0.040	−0.0293	−0.6209	0.535	17	1904784	HIC1	NM_006497	TSS1500	chr17:1952919-1962328	Island
cg04414274	−0.387 ± 0.052	−0.0667	−1.4147	0.1579	17	1904616	HIC1	NM_006497	TSS1500	chr17:1952919-1962328	Island
cg04962428	−0.406 ± 0.079	**−0.1102**	**−2.3475**	**0.01933**	17	1904498	HIC1	NM_006497	TSS1500	chr17:1952919-1962328	Island
cg05445638	−0.473 ± 0.029	−0.0465	−0.9861	0.3246	17	1904920	HIC1;HIC1	NM_001098202;NM_006497	TSS1500;TSS1500	chr17:1952919-1962328	Island
cg06065141	−0.423 ± 0.075	−0.0234	−0.4961	0.62	17	1903911	HIC1	NM_006497	TSS1500	chr17:1952919-1962328	Island
cg09633973	−0.402 ± 0.089	−0.0041	−0.0874	0.9304	17	1904115	HIC1	NM_006497	TSS1500	chr17:1952919-1962328	Island
cg10530104	−0.449 ± 0.023	−0.0444	−0.9402	0.3476	17	1904772	HIC1	NM_006497	TSS1500	chr17:1952919-1962328	Island
cg10948797	−0.358 ± 0.106	−0.0506	−1.0731	0.2838	17	1904357	HIC1	NM_006497	TSS1500	chr17:1952919-1962328	Island
cg11144056	−0.428 ± 0.113	−0.0280	−0.5931	0.5534	17	1904160	HIC1	NM_006497	TSS1500	chr17:1952919-1962328	Island
cg11190071	−0.414 ± 0.095	**−0.1114**	**−2.3723**	**0.0181**	17	1905601	HIC1;HIC1	NM_001098202;NM_006497	TSS1500;5'UTR	chr17:1952919-1962328	Island
cg13254898	−0.419 ± 0.020	−0.0733	−1.5553	0.1206	17	1904544	HIC1	NM_006497	TSS1500	chr17:1952919-1962328	Island
cg13389502	0.154 ± 0.139	0.0882	1.8742	0.06155	17	1908190	HIC1;HIC1	NM_001098202;NM_006497	Body;Body	chr17:1952919-1962328	Island
cg13915354	−0.364 ± 0.074	−0.0653	−1.3841	0.167	17	1904421	HIC1	NM_006497	TSS1500	chr17:1952919-1962328	Island
cg13951527	−0.376 ± 0.083	−0.0780	−1.6562	0.09838	17	1903966	HIC1	NM_006497	TSS1500	chr17:1952919-1962328	Island
cg14809226	−0.405 ± 0.094	−0.0323	−0.6833	0.4947	17	1903723	HIC1	NM_006497	TSS1500	chr17:1952919-1962328	Island
cg16011800	−0.456 ± 0.023	0.0221	0.4669	0.6408	17	1905228	HIC1;HIC1;HIC1	NM_001098202;NM_006497;NM_006497	TSS1500;1stExon;5'UTR	chr17:1952919-1962328	Island
cg16079396	−0.419 ± 0.087	−0.0181	−0.3836	0.7015	17	1903913	HIC1	NM_006497	TSS1500	chr17:1952919-1962328	Island
cg16899486	−0.441 ± 0.024	−0.0363	−0.7680	0.4429	17	1904582	HIC1	NM_006497	TSS1500	chr17:1952919-1962328	Island
cg17029019	−0.275 ± 0.201	−0.0997	−2.1218	0.0344	17	1905874	HIC1;HIC1	NM_001098202;NM_006497	TSS1500;5'UTR	chr17:1952919-1962328	Island
cg17171962	−0.480 ± 0.017	0.0125	0.2651	0.791	17	1904914	HIC1;HIC1	NM_001098202;NM_006497	TSS1500;TSS1500	chr17:1952919-1962328	Island
cg17182507	−0.428 ± 0.083	−0.0372	−0.7880	0.4311	17	1903981	HIC1	NM_006497	TSS1500	chr17:1952919-1962328	Island
cg17210604	−0.421 ± 0.046	−0.0262	−0.5554	0.5789	17	1904867	HIC1;HIC1	NM_001098202;NM_006497	TSS1500;TSS1500	chr17:1952919-1962328	Island
cg17416280	−0.440 ± 0.109	−0.0263	−0.5565	0.5781	17	1904144	HIC1	NM_006497	TSS1500	chr17:1952919-1962328	Island
cg17739038	−0.416 ± 0.118	−0.0586	−1.2433	0.2144	17	1904246	HIC1	NM_006497	TSS1500	chr17:1952919-1962328	Island
cg18051461	−0.432 ± 0.072	−0.0429	−0.9085	0.3641	17	1904823	HIC1	NM_006497	TSS1500	chr17:1952919-1962328	Island
cg19001794	−0.451 ± 0.018	−0.0091	−0.1916	0.8482	17	1904912	HIC1;HIC1	NM_001098202;NM_006497	TSS1500;TSS1500	chr17:1952919-1962328	Island
cg19058189	−0.379 ± 0.064	−0.0045	−0.0944	0.9248	17	1904840	HIC1	NM_006497	TSS1500	chr17:1952919-1962328	Island
cg19962565	−0.466 ± 0.047	−0.0188	−0.3982	0.6907	17	1903714	HIC1	NM_006497	TSS1500	chr17:1952919-1962328	Island
cg20664636*	−0.008 ± 0.207	**−0.1821**	**−3.9190**	**0.0001028**	17	1906346	HIC1;HIC1	NM_001098202;NM_006497	TSS200;5'UTR	chr17:1952919-1962328	Island
cg20682981	−0.234 ± 0.094	−0.0704	−1.4935	0.136	17	1909377	HIC1;HIC1	NM_001098202;NM_006497	3'UTR;3'UTR	chr17:1952919-1962328	S_Shore
cg21556389	−0.374 ± 0.085	0.0018	0.0377	0.9699	17	1904120	HIC1	NM_006497	TSS1500	chr17:1952919-1962328	Island

(*continued on next page*)

Table 1 (*continued*)

TargetID	Methylation level	r	t	P value	CHROMOSOME_36	COORDINATE_36	UCSC_REFGENE_NAME	UCSC_REFGENE_ACCESSION	UCSC_REFGENE_GROUP	UCSC_CPG_ISLANDS_NAME	RELATION_TO_UCSC_CPG_ISLAND
cg21854952	−0.164 ± 0.089	0.2518	5.5070	6.162E-08	17	1908528	HIC1;HIC1	NM_001098202;NM_006497	Body;Body	chr17:1952919-1962328	Island
cg21973370	−0.197 ± 0.092	0.0538	1.1410	0.2545	17	1904669	HIC1	NM_006497	TSS1500	chr17:1952919-1962328	Island
cg21994267	−0.404 ± 0.063	−0.0332	−0.7037	0.482	17	1903956	HIC1	NM_006497	TSS1500	chr17:1952919-1962328	Island
cg22151941	−0.462 ± 0.062	−0.0033	−0.0692	0.9449	17	1903816	HIC1	NM_006497	TSS1500	chr17:1952919-1962328	Island
cg22934970	−0.415 ± 0.075	−0.0934	−1.9845	0.04781	17	1904448	HIC1	NM_006497	TSS1500	chr17:1952919-1962328	Island
cg23621097	−0.121 ± 0.087	0.2285	4.9681	9.637E-07	17	1908986	HIC1;HIC1	NM_001098202;NM_006497	3'UTR;3'UTR	chr17:1952919-1962328	Island
cg23882658	−0.324 ± 0.155	**−0.1001**	**−2.1289**	**0.03381**	17	1905882	HIC1;HIC1	NM_001098202;NM_006497	TSS1500;5'UTR	chr17:1952919-1962328	Island
cg24173182	0.148 ± 0.118	0.1375	2.9388	0.003465	17	1908036	HIC1;HIC1	NM_001098202;NM_006497	Body;Body	chr17:1952919-1962328	Island
cg24576620	−0.357 ± 0.093	−0.0517	−1.0962	0.2736	17	1904427	HIC1	NM_006497	TSS1500	chr17:1952919-1962328	Island
cg25053531	−0.451 ± 0.027	−0.0045	−0.0951	0.9243	17	1904987	HIC1;HIC1	NM_001098202;NM_006497	TSS1500;TSS200	chr17:1952919-1962328	Island
cg25365746	−0.447 ± 0.072	−0.0236	−0.5001	0.6172	17	1903986	HIC1	NM_006497	TSS1500	chr17:1952919-1962328	Island
cg25432975	−0.344 ± 0.169	**−0.1013**	**−2.1562**	**0.0316**	17	1905816	HIC1;HIC1	NM_001098202;NM_006497	TSS1500;5'UTR	chr17:1952919-1962328	Island
cg25449542	−0.415 ± 0.111	−0.0663	−1.4067	0.1602	17	1904355	HIC1	NM_006497	TSS1500	chr17:1952919-1962328	Island
cg25520679*	−0.222 ± 0.176	**−0.1310**	**−2.7961**	**0.005395**	17	1905871	HIC1;HIC1	NM_001098202;NM_006497	TSS1500;5'UTR	chr17:1952919-1962328	Island
cg25893992	−0.287 ± 0.092	0.0379	0.8030	0.4224	17	1904676	HIC1	NM_006497	TSS1500	chr17:1952919-1962328	Island

Bold indicates Cpg sites negatively correlated with HIC1 mRNA level and $P < 0.05$.

* $P < 0.01$.

3.2. Loss of HIC1 promotes growth and migration of lung cancer cells in vitro

Our previous study indicated that a higher methylation level in HIC1 promoter was observed in H292, 95-D, A549, NCI-H1975 and LTEP-a-2 cells than normal human fetal lung fibroblast cells MRC-5 and WI-38 [8], we therefore chose H292 and A549 for further analysis. To further disclose the effect of HIC1 on phenotype of lung cancer, we used CRISPR/Cas9 technology to create stable HIC1-knockout H292/A549 lung cancer cell lines. We noted that HIC1 expression in both mRNA and protein level was dramatically decreased in $H292^{sg4}$ and $A549^{sg4}$ cell lines (Fig. 2A). Cell colony assay showed loss of HIC1 promoted cell growth in H292sg4 and A549sg4 cell lines (Fig. 2B). Notable, the ability of migration in these cell lines was also observed to be markedly enhanced compared with the control group respectively (Fig. 2C, D).

3.3. Genes and pathways identified by loss of HIC1

To assay the alternative genes and pathways modulated by HIC1, we used cDNA array to profile the gene expression program in $H292^{sg4}$ and $A549^{sg4}$ cell lines. 56/36 differentially mRNAs with substantially increased or decreased level respectively were noted (2-fold, Fig. 3A). A heatmap consisting of 35 differentially expressed genes was shown in Fig. 3B. Using qRT-PCR assay, we found that downregulated genes including ADAMTS9, DCDC2, FAM46C, ZNF883 and upregulated genes including F2R, MSH6, PAX2 in H292sg4 and A549sg4 cell lines (Fig. 3C, E), was the potential downstream targets of HIC1, which need to be guaranteed in ongoing study. As shown in Fig. 3D, DNA repair pathway and transcriptional regulation by TP53 pathway were associated with loss of HIC1 expression.

3.4. Loss of HIC1 promotes the occurrence of lung cancer in vivo

To disclose the function of HIC1 in tumorigenesis, three Hic1 sgRNAs were designed to silence HIC1. As shown in Fig. 4A, Hic1_gRNA3 was observed in the most efficient effect on reduction of its expression. pSECC lentiviruses were intratracheally delivered into mouse lungs to delete HIC1 and the lung tissue was analyzed by histopathology (Fig. 4B). Mice infected with sgHIC1-pSECC indicated that HIC1 protein was nearly undetectable compared with sgTd-pSECC infected mice (Fig. 4C). In this case, H&*E*-stained sections showed that the tumor numbers were markedly increased in the $Kras^{G12D/+(Lox\text{-}Stop\text{-}Lox)}$/sgHIC1 group compared with the $Kras^{G12D/+(Lox\text{-}Stop\text{-}Lox)}$/sgTd group (Fig. 4D). No obvious tumor formation in the KrasG12D/+/sgTd group was observed in this stage, which is consistent with other group findings including Ji et al. [17], Sánchez-Rivera FJ et al. [18], Zhang et al. [19] and Wu et al. [20]. The data confirm that loss of HIC1 in lung tissue contributes marked effect on the occurrence of lung cancer.

4. Discussion

The tumor suppressor gene HIC1 has been widely documented to play a vital role in the process of a variety of solid tumors development [21,22]. In this investigation, we firstly confirmed the expression pattern of HIC1 was loss in lung cancer patients. Furthermore, loss of HIC1 expression markedly increased proliferation and migration in lung cancer cells. We then found the genes including ADAMTS9, DCDC2, FAM46C, ZNF883, F2R, MSH6 and PAX2 were the potential downstream targets of HIC1. Pathway analysis showed that DNA repair pathway and transcriptional regulation by TP53 pathway had positive correlation with loss of HIC1 mRNA. In addition, *in vivo* experiments showed that loss of HIC1 had a marked effect on promoting lung tumor growth. These results showed loss of HIC1 expression might play a significant role in lung cancer progression.

HIC1 was discovered epigenetic silencing or loss of heterozygosity in a wide variety of tumor types [12]. Actually, HIC1 has been

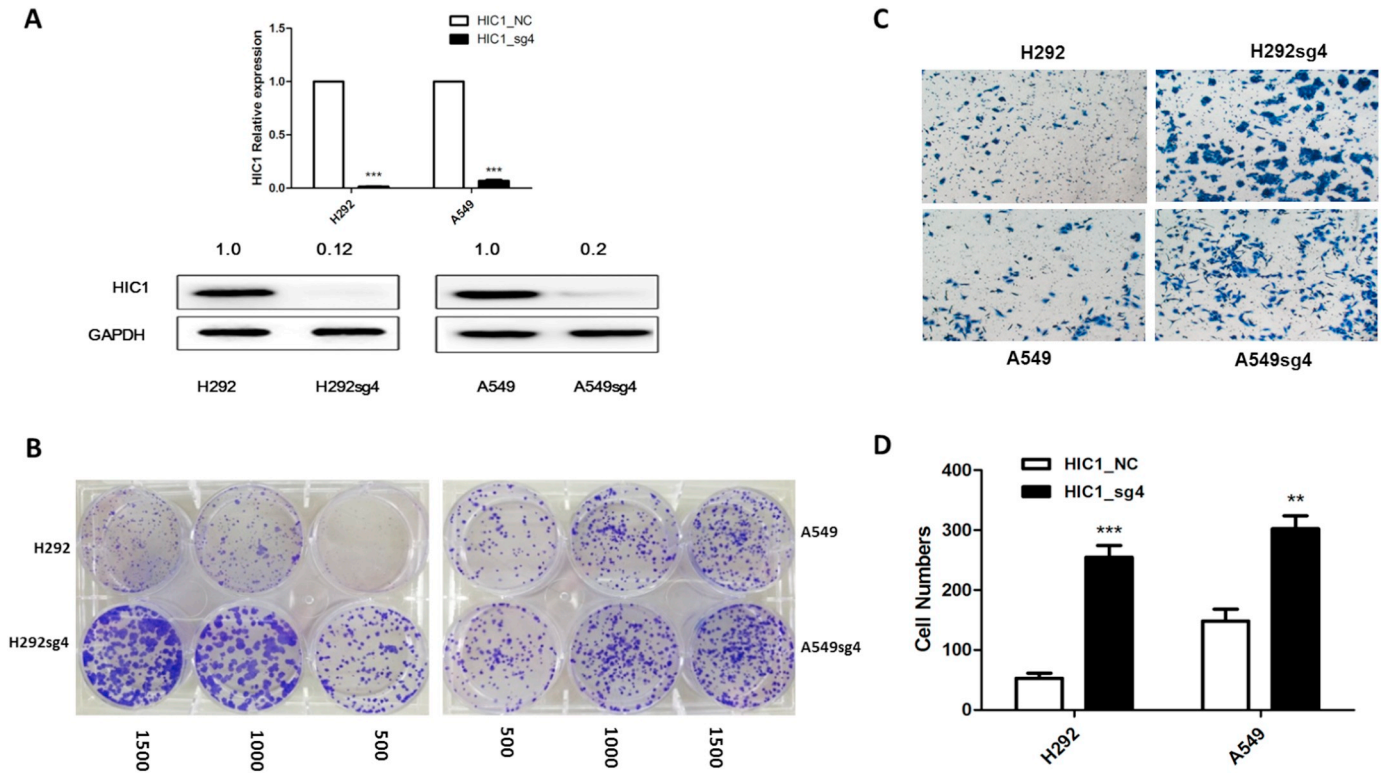

Fig. 2. Loss of HIC1 promotes growth and migration of lung cancer cells. A. CRISPR-Cas9-mediated HIC1 deletion in H292 and A549 lung cancer cells. B. Cell colony assay between H292 and A549 cells and H292sg4 and A549sg4 cells. C. Cell migration assay between H292 and A549 cells and $H292^{sg4}$ and $A549^{sg4}$ cells. D. Quantitative number of migratory cells. $^{**}P < .01$. $^{***}P < .001$. Cell colony assay and cell migration assay were repeated at least three times.

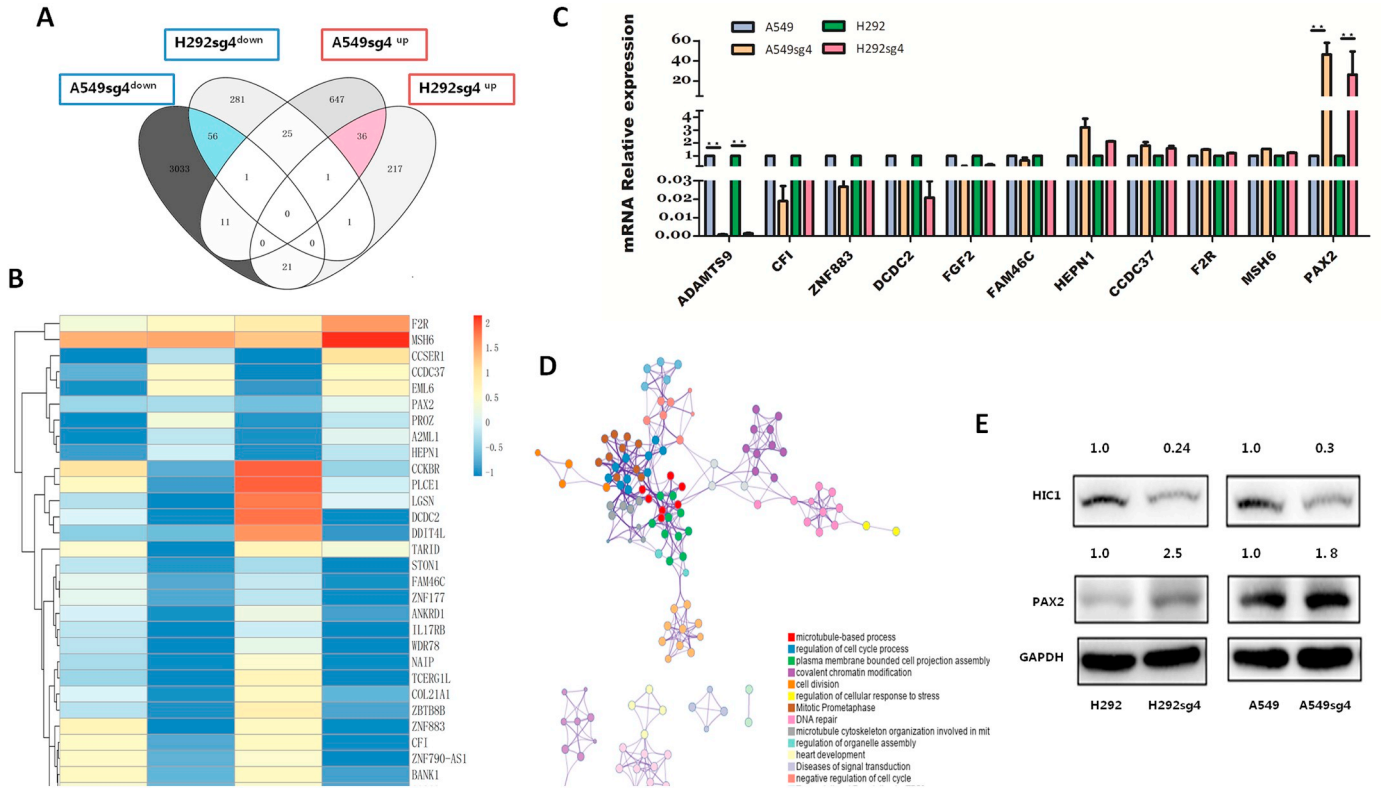

Fig. 3. Genes and Pathways selected by loss of HIC1 expression. A. Differentially mRNA profiling with substantially increased or decreased levels in H292sg4 and A549sg4 cells. B. 35 differentially expressed genes signature in $H292^{sg4}$ and $A549^{sg4}$ cells. C. qPCR validation of differentially expressed genes in $H292^{sg4}$ and $A549^{sg4}$ cells. D. Significant pathway network selected having correlation with HIC1 mRNA downregulation. E. Immunoblot analysis of PAX2 in $H292^{sg4}$ and $A549^{sg4}$ cells. $^{**}P < .01$.

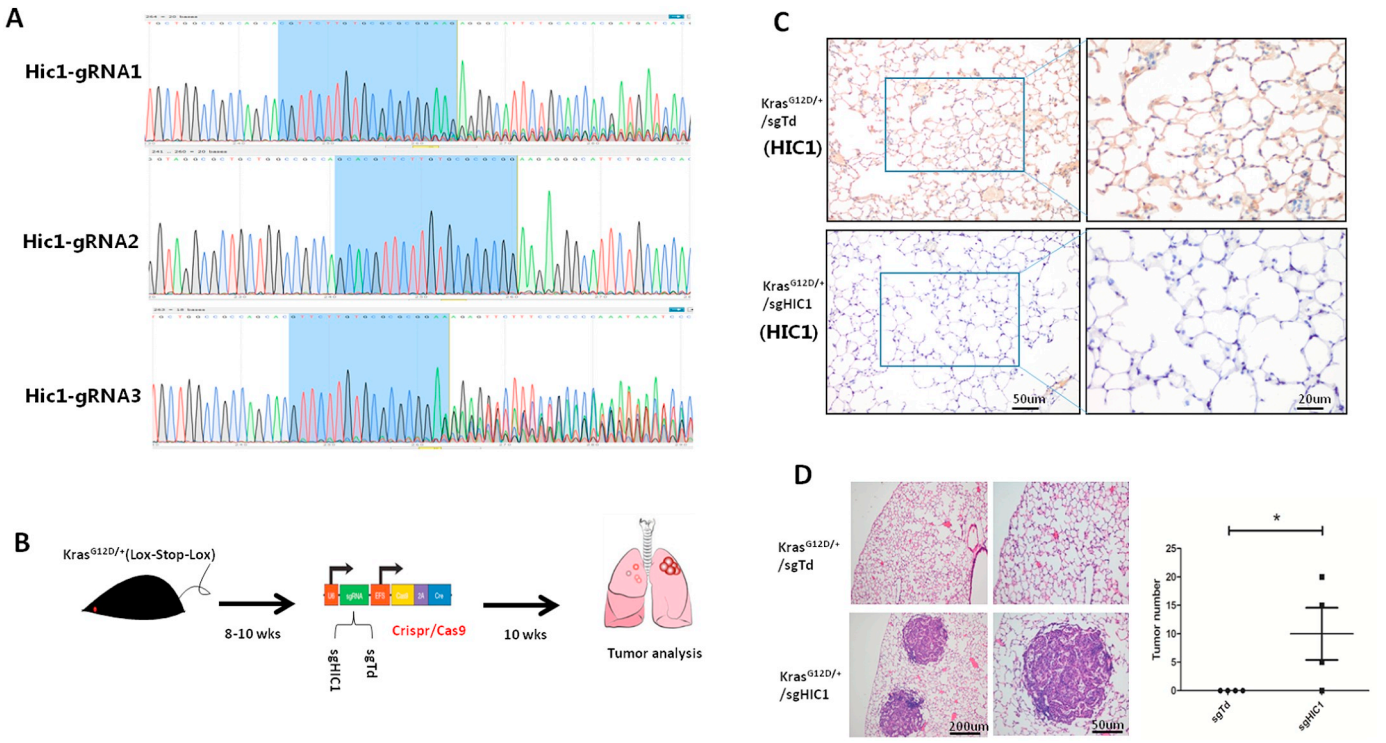

Fig. 4. Loss of HIC1 promotes the occurrence of lung cancer *in vivo*. A. The efficiency of three designed Hic1 sgRNAs. B. Schematic diagram of $Kras^{G12D/+(Lox\text{-}Stop\text{-}Lox)}$/sgHIC1 and $Kras^{G12D/+(Lox\text{-}Stop\text{-}Lox)}$/sgTd mice model construction. C. Representative immunohistochemistry for HIC1 in experimental mice. D. H&E staining of the lung tissues in experimental mice and tumor number in the and $Kras^{G12D/+(Lox\text{-}Stop\text{-}Lox)}$/sgHIC1 group and the $Kras^{G12D/+(Lox\text{-}Stop\text{-}Lox)}$/sgTd group. *P < .05.

systematically studied in our group, which indicates that loss of HIC1 in triple-negative breast cancer (TNBC) and prostate cancer may play a significant role in cancer progression [10,13,14,16]. Recently, we found that a higher methylation level in HIC1 promoter was observed in lung cancer cells and tissues, which was in agreement with Collisson et al.'s findings [23]. Furthermore, studies found that HIC1 could regulate intestinal homeostasis and protective immunity in human intestinal immune system [24]. In line with these findings, we recognized lower expression level of HIC1 in tumor tissues than the corresponding adjacent noncancerous, which was associated with poor outcomes in lung cancer patients. Also, our immunohistochemical analyses data of tissue microarrays (TMAs) in 69 para-carcinoma and 65 carcinoma tissues have shown lower expression level of HIC1 in NSCLC [8]. The mechanism of abnormal expression of HIC1 in cancer progression is under discussion. HIC1 is known as a transcription factor and one important transcriptional target is SIRT1, which could inactivate p53 and establish the Hic1-Sirt1-p53 axis to promote tumor development [7,25,26]. Anette Szczepny et al. demonstrated that loss of HIC1 expression contributed to chromosomal instability in early stage of tumor formation [27]. We found that loss of HIC1 had a positive impact on lung cancer cell proliferation and migration *in vitro* and promote tumor growth *in vivo*. These results were consistent with the fact that loss of HIC1 cooperated with p53 and played a vital role in inducing chromosomal instability in DNA replication [28–30].

We identified ADAMTS9, DCDC2, FAM46C, ZNF883 as downregulated targets and F2R, MSH6, PAX2 as upregulated targets by loss of HIC1. ADAMTS9 is a member of the metalloprotease large family and epigenetically inactivated in breast cancer through blocking EGFR- and TGFβ1/TβR(I/II)-activated AKT signaling [31] ADAMTS9 also functions as a tumor suppressor gene in colorectal cancer by regulating Akt/p53 signaling [32]. DCDC2 is the target gene of miR-645 and downregulation of microRNA-645 suppresses breast cancer cell metastasis [33]. FAM46C is a poly(A) polymerase and its loss of function drives multiple myeloma through the destabilization of ER response transcripts [34]. FAM46C expression level is low in cases and is a potential biomarker to predict hepatic recurrence [35]. ZNF883 is deregulated in five resistant tumors and acted as drivers of the acquired cisplatin resistance [36]. F2R is a 7-transmembrane receptor involved in the regulation of thrombotic response. Proteolytic cleavage leads to the activation of the receptor. According to Lin c, F2R (PAR-1) in NSCLC is mainly expressed on cells that constitute the pulmonary tumor microenvironment, including vascular endothelial cells, macrophages and stromal fibroblasts [[37]]. The human MutS homologue 6 protein (hMSH6), was first reported in 1995 as a G:T binding partner (GTBP) of hMSH2, forming the hMutSα mismatch-binding complex. Molecular mechanisms and cellular regulation of individual MMR proteins are now areas of intensive research [38]. PAX (Paired Box) genes are a family of nine nuclear transcription factors that play a crucial role in various developmental programs, most of the PAX genes are silent in adults. However, they become selectively active during tissue repair and regeneration. Interestingly, several PAX genes have been reported to be expressed in various cancers and likely to contribute to tumorigenesis [39]. Recent studies showed that matrine might suppress the migration and invasion of NSCLCs by inhibiting EMT *via* PAX2 [40]. Taken together, our cDNA assays results showed that ADAMTS9, DCDC2, FAM46C, ZNF883, F2R, MSH6 and PAX2 were identified as the potential downstream targets of HIC1. These results reveal that loss of HIC1 is positively correlated with those genes, thereby induce cell proliferation and migration.

In conclusion, our results provide supportive evidence that loss of HIC1 is involved in lung cancer development, which highlights the role of HIC1 in lung cancer and provide for its therapy strategy.

Competing interests

The authors declare that they have no conflicts of interest.

Acknowledgments

This work was supported by the National Natural Science

Foundation of China to J.H. Wang (81772806, 81272404) and the Program for Professor of Special Appointment (Eastern Scholar to J, Wang) at Shanghai Institutions of Higher Learning.

Authors' contributions

J.H. Wang, G.H. Fu and L. Chen supervised the experiment. X.L. Weng, Y. Li, and M.F. Yao carried out the *in virto* and IHC experiment. T.Q. Wu, L.Y. Zhang and L. Chen carried out the *in vivo* experiment. X.L. Weng, Y. Li and Y.Y. Wang analyzed and discussed the experimental results. Finally, X.L. Weng and Y. Li wrote the manuscript. All authors approved the final manuscript.

Appendix A. Supplementary data

Supplementary data to this article can be found online at https://doi.org/10.1016/j.cellsig.2018.10.006.

References

[1] R. Siegel, D. Naishadham, A. Jemal, Cancer statistics, 2012, CA Cancer J. Clin. 62 (1) (2012) 10–12.
[2] J. Ferlay, I. Soerjomataram, R. Dikshit, S. Eser, C. Mathers, M. Rebelo, D.M. Parkin, D. Forman, F. Bray, Cancer incidence nd mortality worldwide: sources, methods and major patterns in GLOBOCAN 2012, Int. J. Cancer 136 (5) (2015) E359–E386.
[3] R.S. Herbst, J.V. Heymach, S.M. Lippman, Lung cancer, N. Engl. J. Med. 359 (13) (2008) 1367–1380.
[4] R. Siegel, J. Ma, Z. Zou, A. Jemal, Cancer statistics, 2014, CA Cancer J. Clin. 64 (1) (2014) 9–29.
[5] M.M. Wales, M.A. Biel, W. el Deiry, B.D. Nelkin, J.P. Issa, W.K. Cavenee, S.J. Kuerbitz, S.B. Baylin, p53 activates expression of HIC-1, a new candidate tumour suppressor gene on 17p13.3, Nat. Med. 1 (6) (1995) 570–577.
[6] C. Van Rechem, G. Boulay, S. Pinte, N. Stankovic-Valentin, C. Guerardel, D. Leprince, Differential regulation of HIC1 target genes by CtBP and NuRD, via an acetylation/SUMOylation switch, in quiescent versus proliferating cells, Mol. Cell. Biol. 30 (16) (2010) 4045–4059.
[7] W.Y. Chen, D.H. Wang, R.C. Yen, J. Luo, W. Gu, S.B. Baylin, Tumor suppressor HIC1 directly regulates SIRT1 to modulate p53-dependent DNA-damage responses, Cell 123 (3) (2005) 437–448.
[8] X. Wang, Y. Wang, G. Xiao, J. Wang, L. Zu, M. Hao, X. Sun, Y. Fu, G. Hu, J. Wang, Hypermethylated in cancer 1(HIC1) suppresses non-small cell lung cancer progression by targeting interleukin-6/Stat3 pathway, Oncotarget 7 (21) (2016) 30350–30364.
[9] H. Fujii, M.A. Biel, W. Zhou, S.A. Weitzman, S.B. Baylin, E. Gabrielson, Methylation of the HIC-1 candidate tumor suppressor gene in human breast cancer, Oncogene 16 (16) (1998) 2159–2164.
[10] G. Cheng, X. Sun, J. Wang, G. Xiao, X. Wang, X. Fan, L. Zu, M. Hao, Q. Qu, Y. Mao, Y. Xue, J. Wang, HIC1 silencing in triple-negative breast cancer drives progression through misregulation of LCN2, Cancer Res. 74 (3) (2014) 862–872.
[11] M.G. Carter, M.A. Johns, X. Zeng, L. Zhou, M.C. Zink, J.L. Mankowski, D.M. Donovan, S.B. Baylin, Mice deficient in the candidate tumor suppressor gene Hic1 exhibit developmental defects of structures affected in the Miller-Dieker syndrome, Hum. Mol. Genet. 9 (3) (2000) 413–419.
[12] W.Y. Chen, X. Zeng, M.G. Carter, C.N. Morrell, R.W. Chiu Yen, M. Esteller, D.N. Watkins, J.G. Herman, J.L. Mankowski, S.B. Baylin, Heterozygous disruption of Hic1 predisposes mice to a gender-dependent spectrum of malignant tumors, Nat. Genet. 33 (2) (2003) 197–202.
[13] J. Zheng, J. Wang, X. Sun, M. Hao, T. Ding, D. Xiong, X. Wang, Y. Zhu, G. Xiao, G. Cheng, M. Zhao, J. Zhang, J. Wang, HIC1 modulates prostate cancer progression by epigenetic modification, Clin. Cancer Res. 19 (6) (2013) 1400–1410.
[14] M. Hao, Y. Li, J. Wang, J. Qin, Y. Wang, Y. Ding, M. Jiang, X. Sun, L. Zu, K. Chang, G. Lin, J. Du, V. Korinek, D.W. Ye, J. Wang, HIC1 loss promotes prostate cancer metastasis by triggering epithelial-mesenchymal transition, J. Pathol. 242 (4) (2017) 409–420.
[15] S. Paget, M. Dubuissez, V. Dehennaut, J. Nassour, B.T. Harmon, N. Spruyt, I. Loison, C. Abbadie, B.R. Rood, D. Leprince, HIC1 (hypermethylated in cancer 1) SUMOylation is dispensable for DNA repair but is essential for the apoptotic DNA damage response (DDR) to irreparable DNA double-strand breaks (DSBs), Oncotarget 8 (2) (2017) 2916–2935.
[16] Y. Wang, X. Weng, L. Wang, M. Hao, Y. Li, L. Hou, Y. Liang, T. Wu, M. Yao, G. Lin, Y. Jiang, G. Fu, Z. Hou, X. Meng, J. Lu, J. Wang, HIC1 deletion promotes breast cancer progression by activating tumor cell/fibroblast crosstalk, J. Clin. Invest. (2018 Sep 11), https://doi.org/10.1172/JCI99974 (In press).
[17] H. Ji, M.R. Ramsey, D.N. Hayes, C. Fan, K. McNamara, P. Kozlowski, C. Torrice, M.C. Wu, T. Shimamura, S.A. Perera, M.C. Liang, D. Cai, G.N. Naumov, L. Bao, C.M. Contreras, D. Li, L. Chen, J. Krishnamurthy, J. Koivunen, L.R. Chirieac, R.F. Padera, R.T. Bronson, N.I. Lindeman, D.C. Christiani, X. Lin, G.I. Shapiro, P.A. Jänne, B.E. Johnson, M. Meyerson, D.J. Kwiatkowski, D.H. Castrillon, N. Bardeesy, N.E. Sharpless, K.K. Wong, LKB1 modulates lung cancer differentiation and metastas, Nature 448 (2007) 807–810.
[18] F.J. Sánchez-Rivera, T. Papagiannakopoulos, R. Romero, T. Tammela, M.R. Bauer, A. Bhutkar, N.S. Joshi, L. Subbaraj, R.T. Bronson, W. Xue, T. Jacks, Rapid modelling of cooperating genetic events in cancer through somatic genome editing, Nature 516 (2014) 428–431.
[19] W. Zhang, Y. Gao, F. Li, X. Tong, Y. Ren, X. Han, S. Yao, F. Long, Z. Yang, H. Fan, L. Zhang, H. Ji, YAP promotes malignant progression of Lkb1-deficient lung adenocarcinoma through downstream regulation of survivin, Cancer Res. 75 (2015) 4450–4457.
[20] Q. Wu, Y. Tian, J. Zhang, X. Tong, H. Huang, S. Li, H. Zhao, Y. Tang, C. Yuan, K. Wang, Z. Fang, L. Gao, X. Hu, F. Li, Z. Qin, S. Yao, T. Chen, H. Chen, G. Zhang, W. Liu, Y. Sun, L. Chen, K. Wong, K. Ge, L. Chen, H. Ji, In vivo CRISPR screening unveils histone demethylase UTX as an important epigenetic regulator in lung tumorigenesis, Proc. Natl. Acad. Sci. U. S. A. 115 (2018) 3978–3986.
[21] B.R. Rood, H. Zhang, D.M. Weitman, P.H. Cogen, Hypermethylation of HIC-1 and 17p allelic loss in medulloblastoma, Cancer Res. 62 (13) (2002) 3794–3797.
[22] J.K. Stephen, K.M. Chen, V. Shah, S. Havard, A. Kapke, M. Lu, M.S. Benninger, M.J. Worsham, DNA hypermethylation markers of poor outcome in laryngeal cancer, Clin. Epigenetics 1 (1–2) (2010) 61–69.
[23] Cancer Genome Atlas Research Network, Comprehensive molecular profiling of lung adenocarcinoma, Nature 511 (2014) 543–550.
[24] K. Burrows, F. Antignano, A. Chenery, M. Bramhall, V. Korinek, T.M. Underhill, C. Zaph, HIC1 links retinoic acid signalling to group 3 innate lymphoid cell-dependent regulation of intestinal immunity and homeostasis, PLoS Pathog. 14 (2) (2018) e1006869.
[25] J. Luo, A.Y. Nikolaev, S. Imai, D. Chen, F. Su, A. Shiloh, L. Guarente, W. Gu, Negative control of p53 by Sir2alpha promotes cell survival under stress, Cell 107 (2) (2001) 137–148.
[26] R.C. Tseng, C.C. Lee, H.S. Hsu, C. Tzao, Y.C. Wang, Distinct HIC1-SIRT1-p53 loop deregulation in lung squamous carcinoma and adenocarcinoma patients, Neoplasia 11 (8) (2009) 763–770.
[27] A. Szczepny, K. Carey, L. McKenzie, W.S.N. Jayasekara, F. Rossello, A. Gonzalez-Rajal, A.S. McCaw, D. Popovski, D. Wang, A.J. Sadler, A. Mahar, P.A. Russell, G. Wright, R.A. McCloy, D.J. Garama, D.J. Gough, S.B. Baylin, A. Burgess, J.E. Cain, D.N. Watkins, The tumor suppressor Hic1 maintains chromosomal stability independent of Tp53, Oncogene 37 (14) (2018) 1939–1948.
[28] W. Chen, T.K. Cooper, C.A. Zahnow, M. Overholtzer, Z. Zhao, M. Ladanyi, J.E. Karp, N. Gokgoz, J.S. Wunder, I.L. Andrulis, A.J. Levine, J.L. Mankowski, S.B. Baylin, Epigenetic and genetic loss of Hic1 function accentuates the role of p53 in tumorigenesis, Cancer Cell 6 (4) (2004) 387–398.
[29] V. Dehennaut, D. Leprince, Implication of HIC1 (Hypermethylated in Cancer 1) in the DNA damage response, Bull. Cancer 96 (11) (2009) E66–E72.
[30] V. Dehennaut, I. Loison, M. Dubuissez, J. Nassour, C. Abbadie, D. Leprince, DNA double-strand breaks lead to activation of hypermethylated in cancer 1 (HIC1) by SUMOylation to regulate DNA repair, J. Biol. Chem. 288 (15) (2013) 10254–10264.
[31] B. Shao, Y. Feng, H. Zhang, F. Yu, Q. Li, C. Tan, H. Xu, J. Ying, L. Li, D. Yang, W. Peng, J. Tang, S. Li, G. Ren, Q. Tao, T. Xiang, The 3p14.2 tumour suppressor ADAMTS9 is inactivated by promoter CpG methylation and inhibits tumour cell growth in breast cancer, J. Cell. Mol. Med. 22 (2) (2018) 1257–1271.
[32] L. Chen, J. Tang, Y. Feng, S. Li, Q. Xiang, X. He, G. Ren, W. Peng, T. Xiang, ADAMTS9 is Silenced by Epigenetic Disruption in Colorectal Cancer and Inhibits Cell Growth and Metastasis by Regulating Akt/p53 Signaling, Cell. Physiol. Biochem. 44 (4) (2017) 1370–1380.
[33] Y. Cai, W.F. Li, Y. Sun, K. Liu, Downregulation of microRNA-645 suppresses breast cancer cell metastasis via targeting DCDC2, Eur Rev Med Pharmacol Sci 21 (18) (2017) 4129–4136.
[34] S. Mroczek, J. Chlebowska, T.M. Kulinski, O. Gewartowska, J. Gruchota, D. Cysewski, V. Liudkovska, E. Borsuk, D. Nowis, A. Dziembowski, The non-canonical poly(a) polymerase FAM46C acts as an onco-suppressor in multiple myeloma, Nat. Commun. 8 (1) (2017) 619.
[35] H. Tanaka, M. Kanda, D. Shimizu, C. Tanaka, D. Kobayashi, M. Hayashi, N. Iwata, S. Yamada, T. Fujii, G. Nakayama, H. Sugimoto, M. Fujiwara, Y. Niwa, Y. Kodera, FAM46C Serves as a Predictor of Hepatic Recurrence in patients with Resectable Gastric Cancer, Ann. Surg. Oncol. 24 (11) (2017) 3438–3445.
[36] J.M. Piulats, A. Vidal, F.J. Garcia-Rodriguez, C. Munoz, M. Nadal, C. Moutinho, M. Martinez-Iniesta, J. Mora, A. Figueras, E. Guino, L. Padulles, A. Aytes, D.G. Mollevi, S. Puertas, C. Martinez-Fernandez, W. Castillo, M. Juliachs, V. Moreno, P. Munoz, M. Stefanovic, M.A. Pujana, E. Condom, M. Esteller, J.R. Germa, G. Capella, L. Farre, A. Morales, F. Vinals, X. Garcia-Del-Muro, J. Ceron, A. Villanueva, Orthoxenografts of testicular germ cell tumors demonstrate genomic changes associated with cisplatin resistance and identify PDMP as a resensitizing agent, Clin. Cancer Res. 24 (15) (2018 Aug 1) 3755–3766.
[37] C. Lin, C.J. Majoor, J.J.T.H. Roelofs, M.D. de Kruif, H.M. Horlings, K. Borensztajn, C.A. Spek, Potential importance of protease activated receptor (PAR)-1 expression in the tumor stroma of non-small-cell lung cancer, BMC Cancer 17 (1) (2017 Feb 7) 113.
[38] Michael A. Edelbrock, Saravanan Kaliyaperumal, Kandace J. Williams, Structural, molecular and cellular functions of MSH2 and MSH6 during DNA mismatch repair, damage signaling and other noncanonical activities, Mutat. Res. 0 (2013 Mar-Apr) 53–66.
[39] E.J. Robson, S.J. He, M.R. Eccles, A PANorama of PAX genes in cancer and development, Nat. Rev. Cancer 6 (2006) 52–62.
[40] J. Yang, D. He, Y. Peng, H. Zhong, Y. Deng, Z. Yu, C. Guan, Y. Zuo, Z. Xu, Matrine suppresses the migration and invasion of NSCLC cells by inhibiting PAX2-induced epithelial-mesenchymal transition, Onco Targets Ther. 10 (2017) 5209–5217.